Colloids and Surfaces A 579 (2019) 123692

Contents lists available at ScienceDirect

Colloids and Surfaces A

journal homepage: www.elsevier.com/locate/colsurfa

How the interaction between styrene-butadiene-rubber (SBR) binder and a secondary fluid affects the rheology, microstructure and adhesive properties of capillary-suspension-type graphite slurries used for Li-ion battery anodes

Jieun Park[a], Norbert Willenbacher[b], Kyung Hyun Ahn[a,*]

[a] School of Chemical and Biological Engineering, Seoul National University, 08826 Seoul, Republic of Korea
[b] Institute for Mechanical Process Engineering and Mechanics, Karlsruhe Institute of Technology, Gotthard-Franz-Str. 3, 76131 Karlsruhe, Germany

GRAPHICAL ABSTRACT

Here, we investigate how SBR particles, frequently used as a binder in graphite slurries, affect the structure and flow of the wet paste as well as the adhesion of the dry anode layer. We revealed that the SBR particles are located at the interface of both liquid phases, and the amount of added SBR and the energy input for dispersing the secondary fluid offer extra degrees of freedom for adjusting the flow properties and microstructure according to processing and product demands. Most importantly, at a given SBR content, the adhesion strength of the capillary-suspension-type graphite slurries to the current collector is substantially higher than for the anode layers made from conventional suspensions.

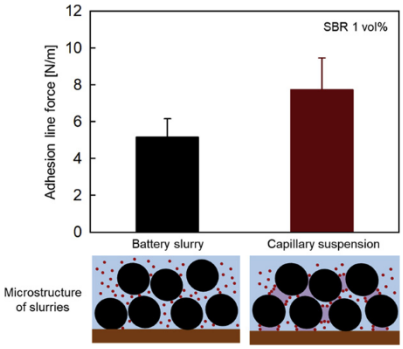

ARTICLE INFO

Keywords:
Capillary suspension
Lithium-ion batteries
Electrode adhesion
Slurry viscosity
Microstructure

ABSTRACT

The distinct structure and flow properties of capillary suspensions, i.e., ternary solid/fluid/fluid systems including two immiscible fluids, make these kinds of slurries promising candidates for the fabrication of Li-ion battery electrodes. Recently, aqueous graphite slurries have been introduced that have beneficial coating properties and yield high-capacity cells with a superior electrochemical performance. Here, we investigate how SBR particles, frequently used as a binder in graphite slurries, affect the structure and flow of the wet paste as well as the adhesion of the dry anode layer. Combining rheological, interfacial and structural investigations revealed that the SBR particles are located at the interface of both liquid phases, and the amount of added SBR and the energy input for dispersing the secondary fluid offer extra degrees of freedom for adjusting the flow properties and microstructure according to processing and product demands. Most importantly, at a given SBR content, the adhesion strength of the capillary-suspension-type graphite slurries to the current collector is substantially higher than for the anode layers made from conventional suspensions. This novel approach promises battery electrodes with extended durability at a low binder content and improved electrical conductivity.

* Corresponding author.
E-mail address: ahnnet@snu.ac.kr (K.H. Ahn).

https://doi.org/10.1016/j.colsurfa.2019.123692
Received 3 May 2019; Received in revised form 16 July 2019; Accepted 17 July 2019
Available online 19 July 2019
0927-7757/

Further research on this highly technical highly demanding topic is needed to understand the underlying physics and its impact on electrochemical cell performance.

1. Introduction

The term *capillary suspension* refers to suspensions whose microstructure is dominated by capillary forces. Such suspensions are ternary systems consisting of two immiscible liquids, called the bulk fluid and the secondary fluid, and solid particles. The flow behavior of a suspension substantially changes when a small amount of immiscible secondary fluid is introduced due to capillary forces inducing self-assembly of a sample spanning the network structure [1,2].

Two distinct states of capillary suspensions have been observed, the so-called pendular and capillary states. The pendular state refers to the state where the secondary fluid wets the particles better than the bulk fluid. In this case, the secondary fluid creates pendular shaped liquid bridges between particles inducing a capillary force-driven network structure in the suspension. In the capillary state, the secondary fluid wets particles less than the bulk fluid. In this case, particle clusters form around small secondary fluid droplets because these configurations are energetically favored. Then, these clusters self-assemble into a percolating network structure [3,4].

Network formation suppresses sedimentation of the particles and improves the suspension stability, but it also alters the rheological properties of the suspension drastically. The addition of a secondary fluid leads to an increase in the yield stress and a low shear viscosity regardless of the state. Capillary suspensions have also been used as pre-cursors for the fabrication of porous sintering materials with distinct porosity and pore size specifications [5]. Due to their unique flow behavior, they are ideally suited for direct ink writing (DIW) to obtain highly porous cellular ceramic parts with unique specific strengths [6]. Sedimentation stability and atomization behavior could be improved for coke slurries [7]. The film formation of titanium dioxide pastes [8] and the conductivity of nickel and silver pastes for printed electronics were improved when a secondary fluid was introduced [9].

Bitsch et al. applied the concept of capillary suspensions to Li-ion battery slurries, and they were able to improve the surface homogeneity in slot-die coating operations [10]. High capacity graphite electrodes with a superior electrochemical performance were obtained by combining a conventionally prepared anode layer adjacent to the current collectors and a capillary suspension based second layer that included the same particles and binders [11,12]. However, this approach deteriorated the adhesion properties of the battery electrodes by 20–30 %. Adhesion between the electrode layer and current collector is decisive for the battery life time and an important cell performance features [13]. The adhesion strength is tightly related to the type and amount of binder used in the slurries [14–16]. The most common binder for aqueous battery slurries is styrene-butadiene rubber (SBR) latex [17,18]. Therefore, we want to understand how the SBR-latex affects the formation and structure of graphite based capillary-suspension-type slurries that are used in the fabrication of lithium ion battery anodes. Furthermore, we want to elucidate how the specific structure and potential colloidal interactions with other ingredients affect the adhesion performance of the slurries including the SBR binder.

2. Material and methods

2.1. Materials

Capillary suspensions were prepared using components frequently used in a commercial Li-ion battery anode slurry. Synthetic graphite (SMGPA, China Steel Chemical Corporation, Kaohsiung, Taiwan) with a density of 2.2 g/cm^3, average volume-based diameter d_{50} of 8.92 µm and a specific surface area of 2.24 m^2/g was used as a solid phase. An aqueous carboxymethyl cellulose (CMC, CMC2200, Daicel Corporation, Osaka, Japan) solution was used as a bulk fluid. CMC with a degree of substitution $D > 0.8$ and an average molecular weight $M_w = 150{,}000$ g/mol was added to de-ionized water to prepare these solutions. Spherical styrene-butadiene rubber (SBR, TRD2001, JSR Corporation, Tokyo, Japan) with a density of 1.0 g/cm^3, a diameter $d_{SBR} = 180$ nm and 48 wt% solid mass fraction was used as a binder. According to the manufacturer, the SBR binder particles were obtained from emulsion polymerization. A fatty acid surface layer provided stability for the aqueous latex dispersion [19,20]. 1-octanol (Merck Millipore Corporation, Darmstadt, Germany) with a density of 0.83 g/cm^3 was chosen as the secondary fluid because this fatty alcohol is hardly soluble in water. The concentrations of the graphite particles, CMC and 1-octanol in the slurries were 18.85 vol%, 1.56 vol% and 2 vol %, respectively. The volume fraction of the SBR binder particles was adjusted (0.47 vol%, 0.94 vol%, 1.41 vol%, 1.88 vol% and 2.35 vol%) to assess how this binder affects the flow properties of the capillary-suspension-type graphite slurries and the adhesion of the corresponding dry anode layer to the current collector (Table 1).

2.2. Sample preparation

CMC-water solution was prepared by adding 3 wt% of CMC to distilled water. Mixtures were stirred using a propeller type stirrer with a diameter of 50 mm at 1000 rpm (rpm) for 3 h. The CMC-water solution and 18.85 vol% of graphite particles were mixed using a dissolver type stirrer with a diameter of 60 mm at 1500 rpm for 40 min. This highly concentrated suspension was prepared to assure slurry homogeneity and de-agglomeration of the graphite particles. Subsequently, water was added stepwise in three steps at 10 min intervals until the concentration of the CMC polymer reached 1.56 vol%. In this paper, we used the term bulk slurry for this suspension. Battery slurries were prepared by adding the SBR binder to a bulk slurry using a dissolver type mixer (diameter = 40 mm) at 650 rpm for 5 min. Capillary suspensions were formed by adding 2 vol% of 1-octanol using a dissolver type stirrer (diameter = 40 mm) at 1000 rpm for a certain mixing time t_m. The mixing time was varied between 1 min. $< t_m <$ 10 min. The samples were labeled as shown in Table 2.

2.3. Rheological characterization

The rheological properties of the slurries were measured using RheoStress 1 (Thermo Scientific, Germany) and Discovery HR-3 (TA instrument, USA) rotational rheometers equipped with a parallel plate fixture (35 mm in diameter) at 20 °C. All the slurries were subjected to a rest time of 120 s before starting the measurements to exclude the residual stress due to the sample loading process. Viscosity was measured

Table 1
Composition of the investigated graphite slurries. The concentration of the ingredients is given in volume fractions (vol%), and water is added such that the total fraction is 100 vol%.

	graphite	CMC	octanol	SBR
Volume percent [vol %]	18.85	1.56	0	0
			2	0.47
				0.94
				1.41
				1.88
				2.35

Table 2
Labelling of the samples with various amounts of SBR binder or mixing times.

Sample	composition
bulk	graphite/CMC/water
#SBR (battery)	graphite/CMC/water/# vol% SBR
oct	graphite/CMC/water/octanol(2 vol%)
#SBR/oct	graphite/CMC/water/# vol% SBR/oct
#SBR/oct($)	graphite/CMC/water/# vol% SBR/oct (mixing time $ minute)

in steady shear rate sweep tests, covering the shear rate range from 0.01 s^{-1} to 1000 s^{-1}. The complex shear modulus G* = G'+iG" of the slurries was obtained from the frequency sweep tests at frequencies between 0.1 rad/s and 100 rad/s in the linear viscoelastic regime identified in prior stress amplitude sweep tests at 1 rad/s.

2.4. Structure analysis by cryogenic-SEM

The slurry microstructure was characterized using a field emission scanning electron microscope (FE-SEM), a Mira3 LMU (Tescan, Brno – Kohoutovice, Czech Republic). The PP3000 T (Quorum Technologies, Lewes, UK) was used to freeze the samples. The samples as 10 µl aliquots were loaded into the rivet of the shuttle stub and then frozen in liquid nitrogen after putting the shuttle to the bayonet of the transfer device. Frozen samples were transferred to the cryo-preparation chamber, and cut in the cross-sectional direction using a knife inside the pre-chamber. The samples underwent sublimation at −100 °C for 10 min and were then coated with platinum in 10 mA for 120 s. All experiments were conducted at -140 °C. Afterwards, images taken from FE-SEM were analyzed using the MATLAB (The Mathworks Inc.) software. Particle positions were detected by marking the center of the particles, and all particle distances were measured to calculate the 2D-pair correlation function.

2.5. Emulsion formation and characterization of the interfacial properties

An emulsion consisting of 70 vol% water, 29 vol% octanol and 1 vol % SBR binder was observed using optical microscopy (IX-71, Olympus, Japan). Because the water and 1-octanol are both transparent, alcian blue (Sigma Aldrich, USA) was used to dye the water and discriminate it from 1-octanol. All components were mixed using a homogenizer (Ultraturrax, IKA, Germany) at 6000 rpm for 5 min to form the emulsion.

Interfacial tension was measured to examine the effect of the SBR binder at the interface between the bulk and secondary fluid. The pendant drop method was used to measure the interfacial tension between the water including the SBR binder and 1-octanol [21]. A small glass cuvette was filled with 1-octanol, then a drop of water, which contained SBR binder, was injected into it using a syringe with a diameter of 1.65 mm. Time evolution of the droplet shape was assessed using a video camera (AVT Stingray F-033B, Allied Vision Technology: 1/2 CCD, 656 492 square pixels) every 10 s for 20 min. Images were analyzed using commercial software (Drop Shape Analysis, Krüss GmbH, Germany) to calculate the interfacial tension.

The three-phase contact angle refers to the contact angle between the particle and the secondary fluid surrounded by the bulk fluid. This quantity was determined using the sessile drop method. A low-porosity graphite plate (porosity ≤10%, Graphite Cova GmbH, Röthenbach, Germany) was located on the bottom of a transparent cuvette which was filled with the bulk fluid. Then, the secondary fluid was dropped onto the surface of the graphite plate using a syringe. The image of the droplet was taken using a camera (AVT Stingray F-033B), and then, the angle between a drop of the secondary fluid and the graphite plate was analyzed using commercial software (Drop Shape Analysis, Krüss GmbH, Germany).

2.6. Adhesion force measurement

Battery slurries were coated onto a copper foil (10 µm, Itochu Corporation, Japan) used as a current collector for battery anodes and dried to measure the adhesion force between the dried anode layer and the current collector. Slurries were coated using a ZAA 2300 automatic coater (Zehntner GmbH, Switzerland) and a ZUA 2000 doctor blade (Zehntner GmbH, Switzerland) (width $w_B = 60$ mm, thickness $d_B = 300$ µm) at a coating velocity of 50 mm/s. Coated slurries were dried overnight at room temperature. Dried electrodes were then cut to a width of 25 mm and a length of 60 mm. The adhesion force between the electrode layer and the current collector was measured in a 90°-peel test using a TA.XT plus Texture Analyzer (Stable Micro Systems, UK) universal testing machine. The average force needed to peel the battery electrode from the current collector at a speed of 5 mm/s normalized to the width of the specimen was calculated to characterize the adhesive strength in terms of this line force or line load, respectively. All measurements were performed using a load cell with a maximum force of 5 kg and a force sensitivity of 0.1 g.

3. Results and discussion

Herein, we investigated the effect of the SBR binder latex added to capillary suspensions that are used as aqueous anode battery slurries. Graphite was suspended in an aqueous CMC solution, together with 1-octanol added as a secondary fluid. The 3-phase contact angle among the graphite particles, 1-octanol and water was measured to be 82° ± 4°, which suggests that the secondary fluid is located between the particles and forms pendular-shaped bridges. The corresponding strong capillary forces trigger the formation of a sample-spanning network, which we call a capillary network in this paper. This structure formation changes the flow behavior of the suspension dramatically [1]. To understand the effect of the SBR binder on this capillary network, we first investigated the rheological properties of the slurries with and

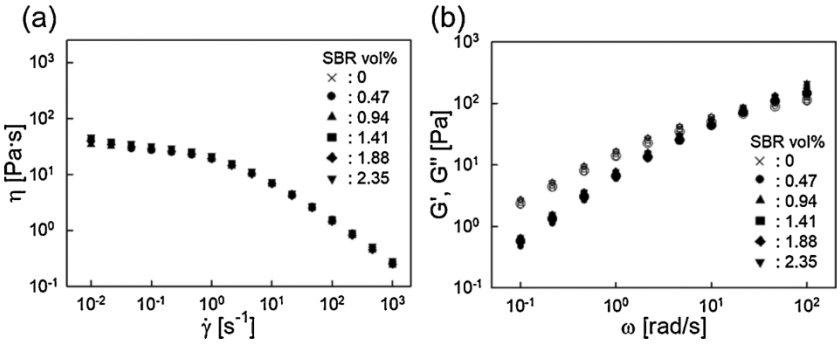

Fig. 1. (a) Viscosity as a function of the shear rate, (b) storage (closed symbol) and loss (open symbol) modulus at 1% strain as a function of the angular frequency of conventional anode battery slurries for various volume fractions of the SBR binder.

without the SBR latex. Then, we focused on the effect of the SBR binder on the adhesion of the dry film to the current collector for films made from regular and capillary-suspension-type slurries with and without the SBR binder.

3.1. Effect of the SBR binder on the rheological properties

Fig. 1 shows the effect of the SBR volume fraction on the rheological properties of the bulk and conventional battery slurries. The bulk slurry refers to a suspension with graphite particles suspended in a CMC-water solution, and the battery slurry refers to the bulk slurry with the SBR binder. Viscosity as a function of the shear rate (a) and the storage and loss moduli (b) as a function of the angular frequency curves all overlap regardless of the volume fraction of the SBR binder. Obviously, the volume fraction of the SBR binder does not affect the rheological properties of the battery slurries in this concentration range of the SBR binder. This result is consistent with findings previously reported by Lim et al. [22]. They found that the SBR binder did not affect the rheological properties of the anode battery slurries unless the CMC concentration, which dominated the flow properties of the battery slurries, was exceptionally low. In contrast, the SBR binder significantly affects the rheological properties of the capillary suspensions shown in Fig. 2a.

Fig. 2 shows the effect of the volume fraction of the SBR binder on the rheological properties of the capillary suspensions. Fig. 2a represents the viscosity change due to the addition of the octanol and SBR binder. The low shear viscosity significantly increased by more than one order of magnitude when the secondary fluid was added to the bulk slurry, whereas the high shear viscosity ($\dot{\gamma} > 100\ s^{-1}$) remained unchanged. The addition of the SBR binder to the capillary suspension reduced the low shear viscosity while the viscosity at the high shear rates remained constant. This viscosity drop is more pronounced at the higher binder volume fractions shown in Fig. 2b. The shear stress at a shear rate of $0.1\ s^{-1}$ gradually decreased from 25 Pa to 13 Pa with the increasing volume fraction of the SBR binder from 0 vol% to 2.35 vol%. This confirms that the strength of the capillary suspension is affected by the SBR binder. The mixing conditions for preparing the capillary suspensions can also affect the strength of the capillary suspension as described in Bosslers et al. [23] and shown in Fig. 3a and b below.

Fig. 3 shows the effect of the mixing time on the rheological properties of capillary suspensions containing the SBR binder. The mixing time Δt is defined as the time during which the octanol was added and mixed. As discussed previously, applying a one minute mixing, $\Delta t = 1$ min., resulted in an increase of the low shear viscosity by more than one order of magnitude. However, the capillary suspension prepared with $\Delta t = 10$ min exhibits a viscosity curve essentially coinciding with that of the conventional slurry without octanol (see Fig. 3a). Fig. 3b shows the drop of the shear stress measured at a constant low shear rate ($\dot{\gamma} = 0.1\ s^{-1}$) with an increasing mixing time for the capillary suspensions that included different fractions of SBR. The drop in the shear stress and hence the viscosity is faster at a higher SBR content. In contrast, no effect from the mixing time is observed for the sample without the SBR binder, and the stress is always higher compared to the samples that included the SBR binder. Bossler et al. reported that the yield stress of the capillary suspensions increased when a longer mixing time was applied until it converged to a constant value [23]. Our results are different and demonstrate that the mixing time can be a critical process parameter when additional SBR particles are present. These particles obviously have a strong impact on the formation of the capillary particle network, but apparently, a strong energy input is required to transport the particles to the interface between the two fluids.

Fig. 4 shows the shear stress at $\dot{\gamma} = 0.1\ s^{-1}$ with different mixing times and mixing speeds for a slurry that included 1.41 vol% SBR. The stress is plotted vs. the total number of stirrer revolutions after adding the octanol to the slurry. This quantity characterizes the mechanical energy input and apparently determines the observed stress and hence the sample microstructure because the data taken for different stirrer speeds fall onto a mastercurve. After about 25,000 revolutions in total, the viscosity level of the slurry without octanol was reached, and no capillary network was maintained.

These results confirm that the total energy input determines the flow behavior of the capillary suspensions if they additionally contain the SBR binder, and this property can be adjusted by selecting the appropriate mixing time and speed. Capillary suspensions containing the 1.41 vol% SBR binder prepared with a mixing time of 1 min at 600 rpm are stable for several weeks and have the same shear stress level even after such a long storage time.

3.2. Structure analysis of the capillary suspensions with the SBR added and different mixing times

Microstructural changes of the capillary suspensions due to the different mixing times were observed directly using a cryogenic scanning electron microscope (cryo-SEM). Fig. 5a–d show cryo-SEM images. Bulk slurry (Fig. 5a), the capillary suspension without SBR binder (Fig. 5b) and capillary suspensions with 1.41 vol% SBR binder prepared with different mixing times (c) $\Delta t = 1$ min (Fig. 5c) and (d) $\Delta t = 10$ min (Fig. 5d) were investigated. Graphite particles, which are shown as white circles, were detected for analyzing the internal structure by calculating a pair correlation function. Fig. 5e shows the pair correlation functions g(r) of the bulk slurry and capillary suspensions with and without the SBR. In the case of the oct, 1.41SBR/oct(1) and 1.41SBR/oct(10) samples, the *g(r)* peaks at the center-to-center distance $r = 7$–8 μm, and then, it approaches one as *r* is further increased. The peak value of 1.41SBR/oct(1) is similar to oct, while 1.41SBR/oct(10) has a lower maximum *g(r)* value than 1.41SBR/oct(1) and oct. No apparent peak can be observed for the bulk slurries containing either the

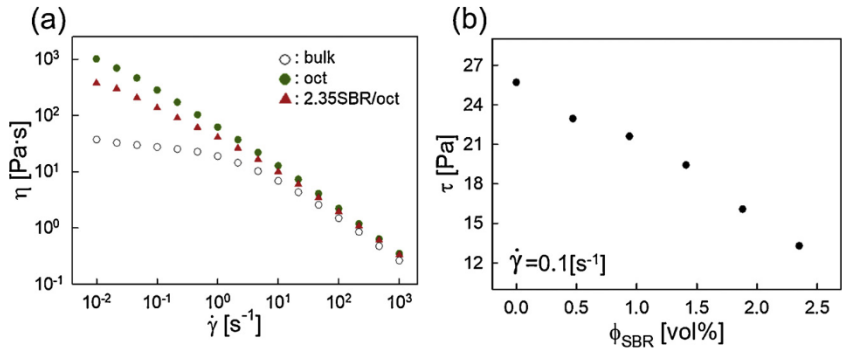

Fig. 2. (a) Viscosity curves of a bulk slurry (open circle) and two capillary suspensions, one with 2 vol% octanol (filled circle) and the other with 2 vol% octanol and 2.35 vol% SBR binder (filled triangle), and (b) shear stress at a constant shear rate of $\dot{\gamma} = 0.1\ s^{-1}$ for the capillary suspensions including various volume fractions of the SBR binder.

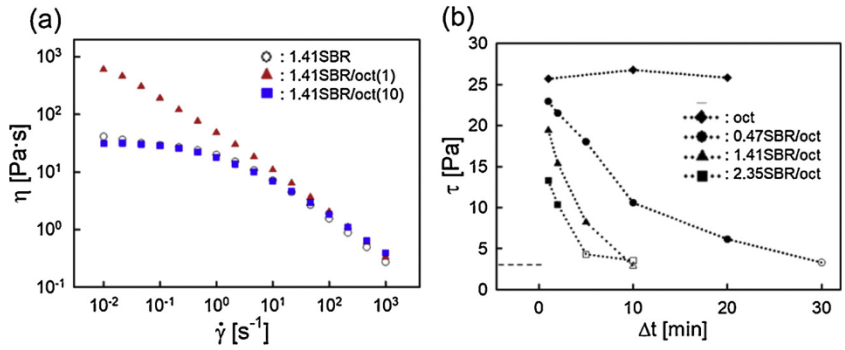

Fig. 3. (a) Viscosity curves of the battery slurry and capillary suspensions containing 1.41 vol% SBR binder prepared with different mixing times, Δt = 1 min. and Δt = 10 min. and (b) shear stress at a fixed shear rate of $\dot{\gamma} = 0.1 s^{-1}$ as a function of the mixing time Δt for various capillary suspensions that included different volume fractions of the SBR binder. Suspensions exhibiting the same viscosity curve as the bulk slurry are marked with open symbols.

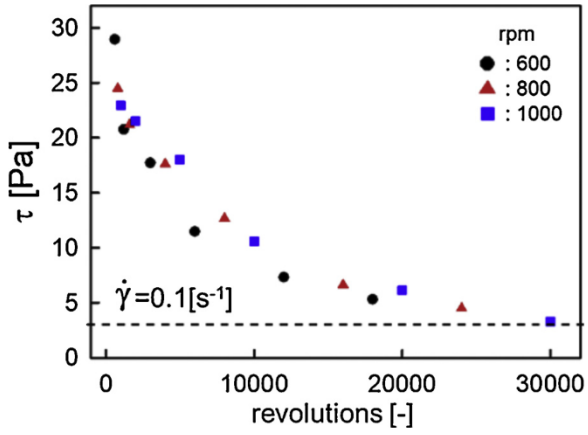

Fig. 4. Shear stress of the capillary suspensions that included 1.41 vol% SBR binder at a shear rate of 0.1 s^{-1} as a function of the revolutions, i.e., the product of the mixing time and speed.

SBR binder or the secondary fluid. The peak position of the pair correlation function *g(r)* resembles the distance between particles in contact, and the absolute value of the *g(r)* maximum characterizes the number of particles in contact. These data shown in Fig. 5e confirm the structure formation already indicated by the high low shear viscosity. A longer mixing time reduces the number of particle contacts, thereby weakening the network structure as already seen in the viscosity data (*see* Fig. 4). Rheological measurements and structure analysis revealed that the particle network structure in the capillary-suspension-type graphite slurries is strongly affected by the volume fraction of the added SBR as well as by the energy input used to create the capillary suspensions.

3.3. Distribution of the SBR particles in the capillary suspension

While a simple mixture of a water and 1-octanol phase separated within minutes Fig. 6 demonstrates that the 1-octanol droplets dispersed in the water were stabilized when the SBR particles were present in the aqueous phase. A mixture of 70 vol% water, 29 vol% 1-octanol and 1 vol% SBR particles split into an upper phase B densely packed with 1-octanol droplets and a lower phase A with a low concentration of 1-octanol droplets. Nevertheless, these droplets were stable in both phases, and we conclude that the SBR binder particles are located at the interface between the two immiscible liquids thus stabilizing the emulsion and preventing coalescence of the dispersed octanol phase. The SBR binder particles consist of hydrophobic polymers, but they are synthesized to have hydrophilic surface groups. Because of this characteristic, they can be wetted by both hydrophobic and hydrophilic liquids, which enables the formation of a Pickering emulsion of octanol in water. In Pickering emulsions, particles are strongly adsorbed at the liquid-liquid interface rather than desorbed into the water or the oil phase [24]. This suggests that the SBR binder particles are also located at the interface of the capillary bridges and surrounding bulk phase in the capillary suspensions that include graphite, water, octanol and SBR. The rheological data and structural analysis presented in sections 3.1 and 3.2 further indicate that the deposition of SBR at this interface strongly depends on the energy input used to add the secondary fluid.

Next, we examined how the SBR binder changes the interfacial tension between water and octanol. As shown in Fig. 7a, the addition of the SBR binder induces a decrease in the interfacial tension with time until a constant value is reached after about 1000s. The SBR particles are 180 nm-sized colloidal particles which diffuse thermally in the medium. Once the SBR particles are localized at the interface, the emulsifier at the surface of the particle lowers the interfacial tension. As time goes on, more SBR particles are gathered at the interface, and thereby decreasing the interfacial tension. Fig. 7b shows the change in

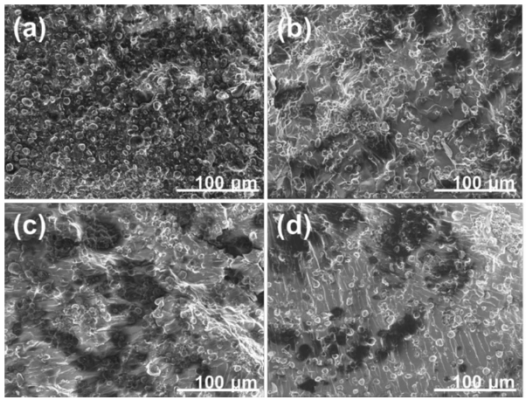

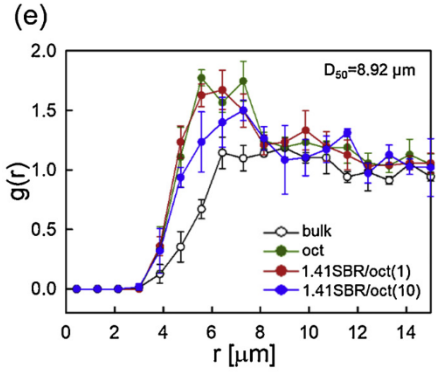

Fig. 5. Cryo-SEM images of the (a) bulk slurry (bulk); (b) the capillary suspension without the SBR binder (oct) and capillary suspension with 1.41 vol% SBR binder prepared with different mixing times (c) Δt = 1 min (1.41SBR/oct(1)) and (d) Δt = 10 min (1.41SBR/oct(10)). Pair correlation functions [7] were plotted as a function of the center-to-center distance r. D_{50} denotes the volume-based average diameter of the graphite particles.

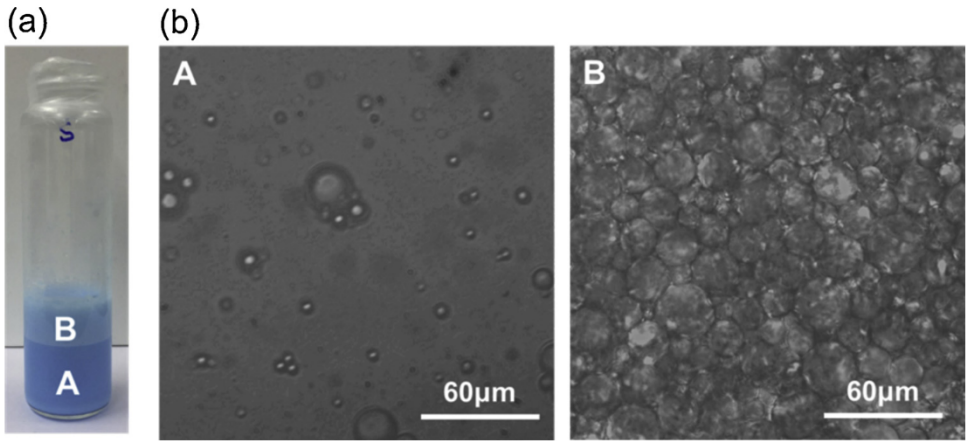

Fig. 6. Mixtures of 70 vol% water, 29 vol% octanol and 1 vol% SBR binder (a). To distinguish the water from the octanol, the water was dyed blue. The sample was mixed at 6000 rpm for 5 min. and left at rest for a day. The photograph on the left shows that the emulsion separated into a lower part (A) with less droplets and an upper part (B) with jammed droplets due to creaming. Light microscopy images of phase A and B are shown on the right (b). (For interpretation of the references to colour in this figure legend, the reader is referred to the web version of this article).

the steady-state interfacial tension with the increasing SBR volume fraction. A higher SBR concentration in water resulted in a higher SBR concentration at the interface, which decreased the interfacial tension.

The capillary force, which dominates the strength of the capillary network structure, is a function of the interfacial tension. The changes in the rheological properties in Figs. 2b and 3 b can be qualitatively attributed to the changes in the capillary forces related to the localization of the SBR particles at the water/octanol interface and the corresponding drop in the interfacial tension.

Diffusion of the SBR particles in the capillary suspension is around 10^6 times slower than in water because of the high viscosity due to the CMC dissolved in the aqueous phase. It seems that the SBR particles in the capillary suspension hardly reach the interface where they are supposed to be located for minimizing the total energy. Applying an external force, especially mixing in this case, increases the probability of locating the SBR particles at the interface. Therefore, a higher mixing energy results in more SBR particles at the interface, decreasing the interfacial tension, thereby weakening the network structure and reducing the level of shear stress at low shear rates.

Fig. 8 shows the microstructure of the capillary suspensions containing 1.41 vol% SBR binder with a mixing time $\Delta t = 1$ min. and $\Delta t = 10$ min. The large raspberry-shaped objects are the graphite particles, and the small white spheres are the SBR particles. The distribution of the SBR particles changed completely when different mixing times were applied. They were observed near the graphite surfaces in the case of $\Delta t = 1$ min, and even a bridge-like SBR structure connecting the graphite particles was observed. Whereas, no SBR particles were found near the graphite particles after $\Delta t = 10$ min.

As discussed previously, the sample prepared with $\Delta t = 1$ min. has a stronger network structure than the $\Delta t = 10$ min. sample. The SBR particles are located in the capillary bridges between the graphite particles when the network structure is strong. Whereas, the sample prepared with $\Delta t = 10$ min. has a weak structure, and no bridges are left.

There seem to be two reasons for the dramatic drop observed in the low shear viscosity when samples were prepared with a long mixing time: the first reason is the reduction of the interfacial energy Γ (cf. Fig. 7), and second one is the reduction of the number of capillary bridges as suggested by the cryo-SEM micrographs (cf. Fig. 5).

Fig. 9 suggests the structures of four different slurries deduced from the results above. When SBR particles are added to the capillary suspension and mixed for a short time, capillary bridges remain and SBR particles are trapped at the interface. Whereas, capillary bridges are destroyed as mixing lasts longer. Mixing accumulates SBR particles at the interface thus reducing the interfacial tensions (see Fig. 7) and finally capillary forces become insufficient to maintain the network structure.

3.4. Adhesion characteristics of the conventional and capillary suspension-type slurries

Fig. 10 shows the adhesion line force F_a of the electrode layers made from the conventional battery slurries without a secondary fluid as a function of the SBR volume fraction. Obviously, the adhesion force strongly increases with the increasing amount of SBR added to the graphite slurry. No measurable adhesion force was found for samples without added SBR.

The adhesion between the electrode layers and the current collector is decisive for the durability of the battery because it maintains the electrical contact between the graphite layers and copper foil when the electrode expands or shrinks while the Li-ions intercalate or de-intercalate into graphite particles during the charging and discharging processes. Therefore, the adhesion force directly correlates with the cycle life of the battery [25,26]. It is generally accepted, that the distribution of the SBR binder determines the adhesion strength of the battery electrode. The adhesion strength becomes stronger as the binder concentration at the interface between the electrode and substrate increases [14,27]. The evidence from the previous sections proves that

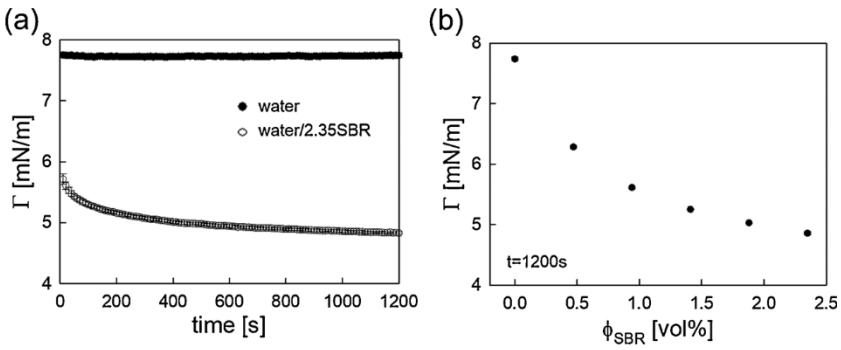

Fig. 7. (a) Interfacial tension measured by the pendant drop method between water and octanol with and without 2.35 vol % SBR binder as a function of time and (b) the dependence of the interfacial tension between water and octanol versus the volume fraction of the SBR binder added to the aqueous phase. Interfacial tension was measured after 1200s when it is considered to have reached an equilibrium state.

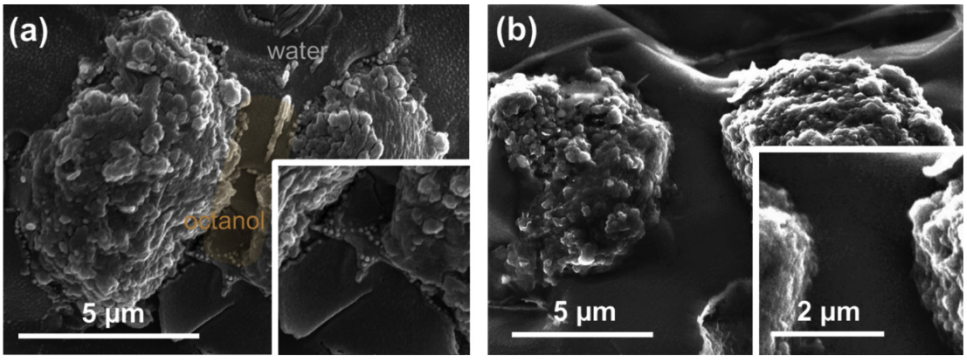

Fig. 8. Cryo-SEM images of the capillary suspensions containing 1.41 vol% SBR binder with different mixing times (a) Δt = 1 min. and (b) Δt = 10 min.

the distribution of the SBR particles can be very different in the capillary suspensions compared to the regular suspensions. Next, we discuss how this affects the adhesion in the corresponding electrodes made from the capillary-suspension-type graphite slurries.

For this comparison, we selected slurries prepared with a mixing time Δt = 1 min. for the added 1-octanol. These slurries were coated onto copper foils and dried as described above. The adhesion measurements were performed, and the results were related to those obtained using the regular battery slurries with the same amount of SBR. The corresponding force ratio, i.e., the adhesion line force F_a of the capillary-suspension-type slurry divided by the line force F_a obtained for the regular battery slurry, is shown in Fig. 11 as a function of the SBR volume fraction ϕ_{SBR}. This force ratio increases with an increasing ϕ_{SBR} and reaches a maximum around ϕ_{SBR} = 1.5 vol% corresponding to an increase in the adhesion force of about 70% for the electrode made from the capillary-suspension-type slurry compared to the one obtained from the regular battery slurry. The force ratio decreases when the SBR fraction is further increased but is still well above the one for the highest SBR content ϕ_{SBR} = 2.35 vol% investigated here.

Fig. 11 shows the scanning electron microscopy (SEM) images of the battery electrode surfaces delaminated from the copper foil. Fig. 12a corresponds to an electrode prepared from a battery slurry without a secondary fluid, whereas the film shown in Fig. 12b was made from a capillary suspension including 2 vol% 1-octanol as a secondary fluid phase. Fig. 12a shows the spherical graphite particles and flattened, smooth polymer regions. In contrast, the film made from the capillary suspension (Fig. 12b) has a less uniform and smooth surface; the polymer regions seem to be ruptured, and several hollow centers are observed.

These SEM images indicate a different failure and delamination characteristic for the electrodes made from the regular and capillary-suspension-type battery slurries. The smooth polymer surface in Fig. 11a indicates an ideal adhesive failure, whereas the irregular polymer pattern visible in Fig. 11b may be due to a partial cohesive failure. This indicates a stronger adhesive strength and thus, is consistent with the results shown in Fig. 10.

One possible reason for this improved adhesion might be a suppression of binder migration often observed during the drying of the regular battery slurries [27–29] During solvent evaporation, a capillary

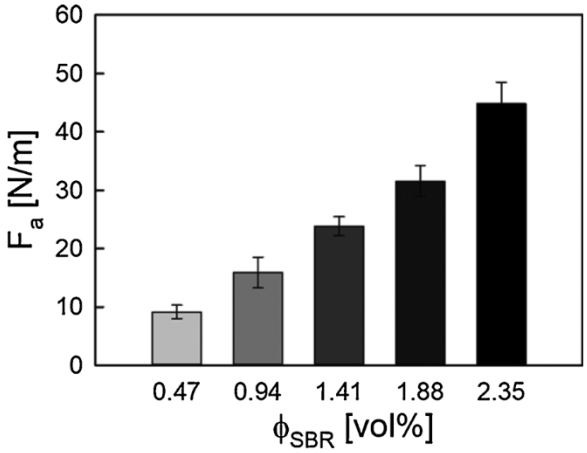

Fig. 10. Adhesion line forces F_a of the battery electrodes measured using the 90°-peel test as a function of the SBR volume fractions.

pressure induced flow carries the binder particles to the surface of the coating layer causing a binder gradient in perpendicular direction and a depletion of the binder close to the current collector thus limiting the adhesion. Such a migration is suppressed in the capillary-suspension-type slurries because the SBR particles are trapped at the water/octanol interface of the capillary bridges between the graphite particles. The lower vapor pressure of octanol (0.087 mbar at 20 °C) compared to water (23.38 mbar at 20 °C) could further prevent binder migration.

Another reason for the strong adhesion of the capillary-suspension-based electrode layers could be related to the preferential wetting of the octanol (0° contact angle on the copper, ideal wetting) compared to water (50° contact angle on the copper as determined by the sessile drop method). Thus, capillary bridges between the graphite particles and the copper foil may form after the coating, which additionally trap the SBR particles at the interface between the electrode layer and current collector. Further investigations are necessary to verify this hypothesis.

However, the improved adhesion of the capillary-suspension-based electrode layers on the current collector is an experimental fact and

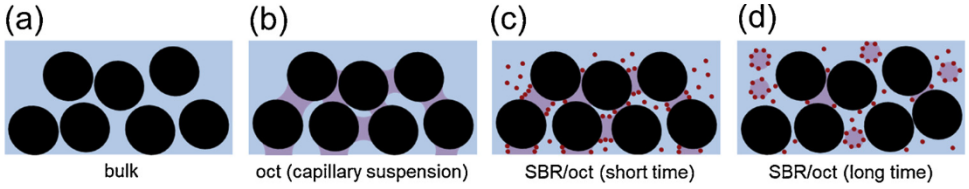

Fig. 9. Schematic of structures for the (a) bulk slurry (bulk); (b) the capillary suspension without the SBR binder (oct) and capillary suspension with SBR binder prepared with (c) short and (d) long mixing times. Large black circles are graphite particles and small red circles are SBR particles. Octanol is shown in violet (dark region between particles in). (For interpretation of the references to colour in this figure legend, the reader is referred to the web version of this article).

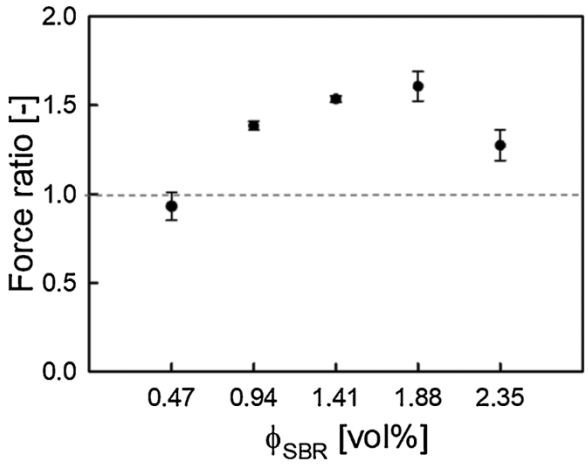

Fig. 11. Dependence of the force ratio defined as the adhesion force from the capillary suspension divided by the adhesion force from battery slurry for various SBR volume fractions.

may enable an improved battery durability at a lower binder content. Further investigations including cell cycling tests will be necessary to validate this.

4. Conclusions

Capillary suspensions are ternary solid/fluid/fluid systems that include two immiscible liquids. Capillary forces in such systems induce the formation of a percolated particle network which results in a paste-like texture and a distinct flow behavior of the suspensions. Recently, this concept has been used to prepare graphite slurries for Li-ion battery anodes with beneficial coating properties [9] and high capacity cells with a superior electrochemical performance [10]. Here, we investigated how additional SBR-particles, widely used as a binder in commercial battery slurries, affect the flow behavior and microstructure of capillary-suspension-type battery slurries that included graphite, an aqueous CMC solution, and 1-octanol as a secondary fluid. Furthermore, we investigated the adhesion of the electrode layers made from such slurries to the current collector.

Our investigations revealed that the particle network, a characteristic for this kind of suspensions, is formed even in the presence of SBR in the aqueous phase. This showed up in a strong, more than one order of magnitude, increase in the low shear viscosity and was directly confirmed by a pronounced peak in the pair correction function at the particle contact deduced from the cryo-SEM images. However, the SBR slightly weakens the structure, and correspondingly, the low shear viscosity decreases with increasing φ_{SBR}, dropping to half the value of the SBR-free slurry when 2.35 vol % SBR is added.

Furthermore, we showed that the energy input during addition of 1-octanol as immiscible, secondary fluid is decisive for structure formation. The strong increase in the low shear viscosity is only achieved at a short mixing time (1 min. mixing time with the equipment used here), but monotonically decreases with increasing energy input, eventually reaching the viscosity level of the slurry without a secondary fluid. Samples with a higher SBR content are more sensitive to the mixing conditions than those with a lower amount of SBR, and the lower viscosity limit is reached faster. Pair correlation functions determined from cryo-SEM images provide direct evidence that there is a reduced number of particle contacts in strongly stirred samples. However, once the slurries are prepared, they are stable for several weeks. Emulsification experiments demonstrated that SBR particles suspended in an aqueous phase can diffuse to the water/octanol interface and stabilize the octanol droplets. The interfacial tension between water and octanol decreased monotonically from 7.74 mN/m to 4.85 mN/m when φ_{SBR} was increased up to 2.35 vol %.

Cryo-SEM images directly show that the SBR particles are located in the contact region between the adjacent graphite particles for the slurries prepared with a low energy input, but not for the slurries made with extended octanol mixing times.

These investigations show that the amount of added SBR and the energy input for mixing the secondary fluid are additional parameters that have to be taken into account when fabricating capillary-suspension-type battery slurries and offer extra degrees of freedom for adjusting the flow properties or microstructure to a desired level.

Finally, we investigated the adhesion of the electrode layers made from capillary-suspension-type graphite slurries to the copper-made current collector as a function of SBR concentration. Generally, the adhesion of the electrodes made from this type of slurry is distinct, i.e., up to 50%, higher than for electrodes made from corresponding slurries that do not include 1-octanol as a secondary fluid. Whether this is due to the suppressed migration of the binder to the surface of the electrode during drying because SBR is trapped in the capillary bridges between graphite particles or whether additional octanol bridges between the copper foil and graphite particles promoted by the preferred wetting of octanol on copper, needs further investigation.

Irrespective of that not yet fully disclosed physical origin of the enhanced adhesion, the capillary suspension concept seems to offer a new approach to achieve Li-ion battery electrodes with extended durability at a lower binder content. This may have additional benefits with respect to the electrode conductivity. Further research including cell cycling tests will be performed to get further insight into this technically highly demanded topic.

Li-ion batteries are highly demanded for further expansion of electric vehicles and storage of fluctuating electrical energy supply from renewable resources. Sustainable large scale deployment of these batteries requests formulation of water-based electrode pastes. The flow behavior of such pastes is important to understand with respect to a tailored processing and coating. The adhesion of corresponding dry layers to the collector foil is decisive for battery lifetime and

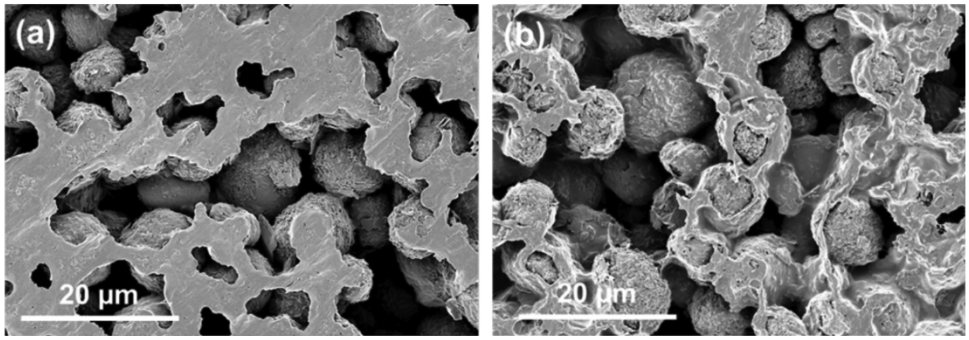

Fig. 12. SEM images of the delaminated surfaces for the battery electrodes at the copper foil (substrate). Battery electrodes were prepared with (a) battery slurry containing 1.41 vol% SBR binder and (b) capillary suspension containing 1.41 vol% SBR binder and 2 vol% octanol.

electrochemical performance. Our study focused on the promising capillary suspension concept for paste formulation. Here we demonstrated how SBR, which is a widely used additive for adhesion promotion in conventional battery slurries, affects the flow behavior of capillary suspension type slurries and the adhesion of the corresponding dry layers to the electrode. Microscopic investigations revealed how the SBR particles modify the water/octanol interface in these slurries. This insight can help to further improve formulation and technical performance of battery electrode slurries but may also stimulate the application of the capillary suspension concept for other slurry based processes and products.

Declaration of Competing Interest

The authors declare that they have no known competing financial interests or personal relationships that could have appeared to influence the work reported in this paper.

Acknowledgements

This work was supported by the National Research Foundation of Korea (NRF) grant funded by the Korea government (MSIT) (No. NRF-2018R1A5A1024127).

References

[1] E. Koos, N. Willenbacher, Capillary forces in suspension rheology, Science 331 (6019) (2011) 897–900 Feb 18.
[2] S.S. Velankar, A non-equilibrium state diagram for liquid/fluid/particle mixtures, Soft Matter 11 (43) (2015) 8393–8403 Nov 21.
[3] E. Koos, Capillary suspensions: particle networks formed through the capillary force, Curr. Opin. Colloid Interface Sci. 19 (6) (2014) 575–584 Dec 1.
[4] F. Bossler, E. Koos, Structure of particle networks in capillary suspensions with wetting and nonwetting fluids, Langmuir 32 (6) (2016) 1489–1501 Feb 16.
[5] J. Dittmann, J. Maurath, B. Bitsch, N. Willenbacher, Highly porous materials with unique mechanical properties from smart capillary suspensions, Adv. Mater. 28 (8) (2016) 1689–1696 Feb 24.
[6] J. Maurath, J. Dittmann, N. Schultz, N. Willenbacher, Fabrication of highly porous glass filters using capillary suspension processing, Sep. Purif. Technol. 149 (2015) 470–478.
[7] L. Jampolski, A. Sänger, T. Jakobs, G. Guthausen, T. Kolb, N. Willenbacher, Improving the processability of coke water slurries for entrained flow gasification, Fuel 185 (2016) 102–111.
[8] M. Schneider, J. Maurath, S.B. Fischer, M. Weiss, N. Willenbacher, E. Koos, Suppressing crack formation in particulate systems by utilizing capillary forces, ACS Appl. Mater. Interfaces 9 (12) (2017) 11095–11105 Mar 29.
[9] M. Schneider, E. Koos, N. Willenbacher, Highly conductive, printable pastes from capillary suspensions, Sci. Rep. 6 (2016) p. 31367, Aug 10.
[10] B. Bitsch, J. Dittmann, M. Schmitt, P. Scharfer, W. Schabel, N. Willenbacher, A novel slurry concept for the fabrication of lithium-ion battery electrodes with beneficial properties, J. Power Sources 265 (2014) 81–90.
[11] B. Bitsch, T. Gallasch, M. Schroeder, M. Börner, M. Winter, N. Willenbacher, Capillary suspensions as beneficial formulation concept for high energy density Li-ion battery electrodes, J. Power Sources 328 (2016) 114–123.
[12] J.-T. Son, E. Cairns, Structure and electrochemical characterization of LiNi0.3Co0.3Mn0.3Fe0.1O2 cathode for lithium secondary battery, J. Korean J. Chem. Eng. 24 (5) (2007) 888–891.
[13] S.L. Chou, Y. Pan, J.Z. Wang, H.K. Liu, S.X. Dou, Small things make a big difference: binder effects on the performance of Li and Na batteries, Phys. Chem. Chem. Phys. 16 (38) (2014) 20347–20359 Oct 14.
[14] W. Haselrieder, B. Westphal, H. Bockholt, A. Diener, S. Höft, A. Kwade, Measuring the coating adhesion strength of electrodes for lithium-ion batteries, Int. J. Adhes. Adhes. 60 (2015) 1–8.
[15] J. Lee, S. Sung, Y. Kim, J.D. Park, K.H. Ahn, A new paradigm of materials processing—heterogeneity control, Curr. Opin. Chem. Eng. 16 (2017) 16–22.
[16] C. Hanisch, T. Loellhoeffel, J. Diekmann, K.J. Markley, W. Haselrieder, A. Kwade, Recycling of lithium-ion batteries: a novel method to separate coating and foil of electrodes, J. Clean. Prod. 108 (2015) 301–311.
[17] B. Son, et al., Measurement and analysis of adhesion property of lithium-ion battery electrodes with SAICAS, ACS Appl. Mater. Interfaces 6 (1) (2014) 526–531 Jan 8.
[18] J.-T. Lee, Y.-J. Chu, X.-W. Peng, F.-M. Wang, C.-R. Yang, C.-C. Li, A novel and efficient water-based composite binder for LiCoO2 cathodes in lithium-ion batteries, J. Power Sources 173 (2) (2007) 985–989.
[19] J.-H. Lee, S. Lee, U. Paik, Y.-M. Choi, Aqueous processing of natural graphite particulates for lithium-ion battery anodes and their electrochemical performance, J. Power Sources 147 (1-2) (2005) 249–255.
[20] J.S. Kim, S. Hong, D.W. Park, S.E. Shim, Water-borne graphene-derived conductive SBR prepared by latex heterocoagulation, Macromol. Res. 18 (6) (2010) 558–565.
[21] J.D. Berry, M.J. Neeson, R.R. Dagastine, D.Y. Chan, R.F. Tabor, Measurement of surface and interfacial tension using pendant drop tensiometry, J. Colloid Interface Sci. 454 (2015) 226–237 Sep 15.
[22] S. Lim, S. Kim, K.H. Ahn, S.J. Lee, The effect of binders on the rheological properties and the microstructure formation of lithium-ion battery anode slurries, J. Power Sources 299 (2015) 221–230.
[23] F. Bossler, L. Weyrauch, R. Schmidt, E. Koos, Influence of mixing conditions on the rheological properties and structure of capillary suspensions, Colloids Surf. A Physicochem. Eng. Asp. 518 (2017) 85–97. Apr 5.
[24] Y. Chevalier, M.-A. Bolzinger, Emulsions stabilized with solid nanoparticles: pickering emulsions, Colloids Surf. A Physicochem. Eng. Asp. 439 (2013) 23–34.
[25] L. Chen, X. Xie, J. Xie, K. Wang, J. Yang, Binder effect on cycling performance of silicon/carbon composite anodes for lithium ion batteries, J. Appl. Electrochem. 36 (10) (2006) 1099–1104.
[26] J.-B. Kim, B.-S. Jun, S.-M. Lee, Improvement of capacity and cyclability of Fe/Si multilayer thin film anodes for lithium rechargeable batteries, Electrochim. Acta 50 (16-17) (2005) 3390–3394.
[27] S. Jaiser, M. Müller, M. Baunach, W. Bauer, P. Scharfer, W. Schabel, Investigation of film solidification and binder migration during drying of Li-Ion battery anodes, J. Power Sources 318 (2016) 210–219.
[28] S. Lim, K.H. Ahn, M. Yamamura, Latex migration in battery slurries during drying, Langmuir 29 (26) (2013) 8233–8244 Jul 2.
[29] S. Lim, S. Kim, K.H. Ahn, S.J. Lee, Stress development of li-ion battery anode slurries during the drying process, Ind. Eng. Chem. Res. 54 (23) (2015) 6146–6155.